Supplementary Data

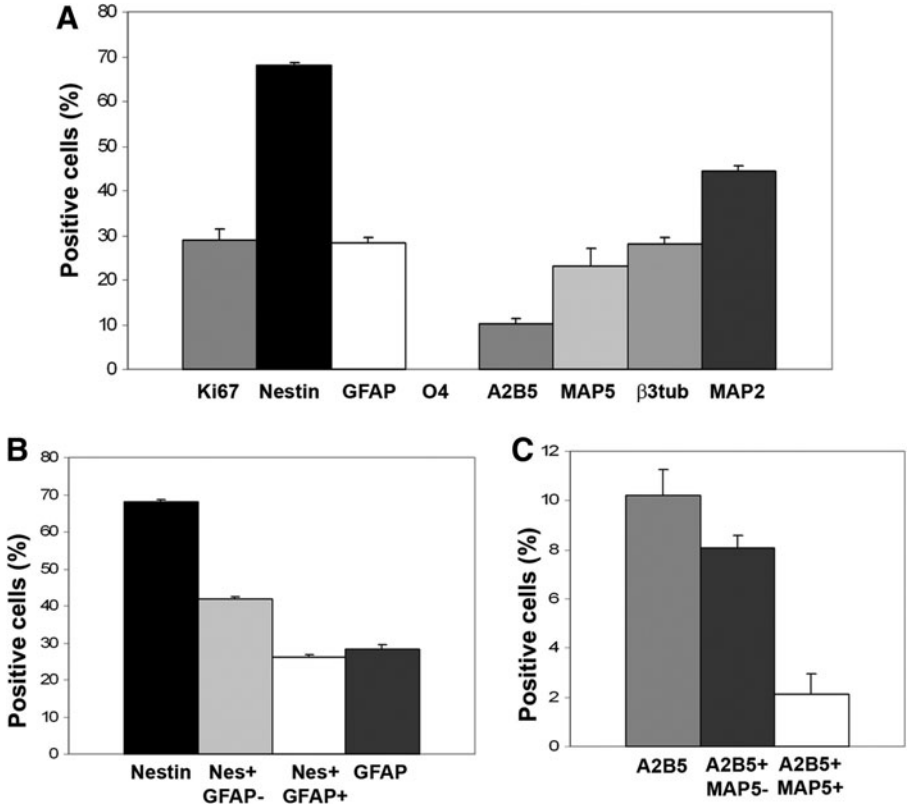

SUPPLEMENTARY FIG. S1. HFC6 cell population is composed of immature neuroepithelial-like cells and committed progenitors from the 3 main CNS lineages. **(A)** Proportions of cells expressing various markers in HFC6 cell population after amplification in vitro (passages 9), expressed as a percentage of total Hoechst$^+$ nuclei ± SEM. HFC6 cells are a heterogeneous population composed of Ki67$^+$ proliferating cells, as well as Nestin$^+$ neuroepithelial-like cells, glial fibrillary acidic protein (GFAP) astrocytes, A2B5$^+$, MAP5$^+$, and β3 Tubulin$^+$ neuroblasts, and MAP2$^+$ mature neurons. No O4$^+$ oligodendrocytes were detected among HFC6 cells. Note that, compared with HFC7 cells, HFC6 cells comprise a higher proportion of neuroepithelial cells and a lower proportion of committed neurons. These differences are probably related to the age of the fetuses. **(B)** As for HFC7 cell population, Nestin$^+$ cell population contains a majority of Nestin$^+$/GFAP$^-$ neuroepithelial-like cells as well as Nestin$^+$/GFAP$^+$ astrocytes. **(C)** Among the A2B5$^+$ cell population, ~1/5 corresponds to A2B5$^+$/MAP5$^+$ neuroblasts, whereas 4/5 are A2B5$^+$/MAP5$^-$ OPCs. HFC, human fetal cortex; hPNC, human neural progenitor cell; CNS, central nervous system; SEM, standard error of the mean; OPC, oligodendrocyte progenitor cell.

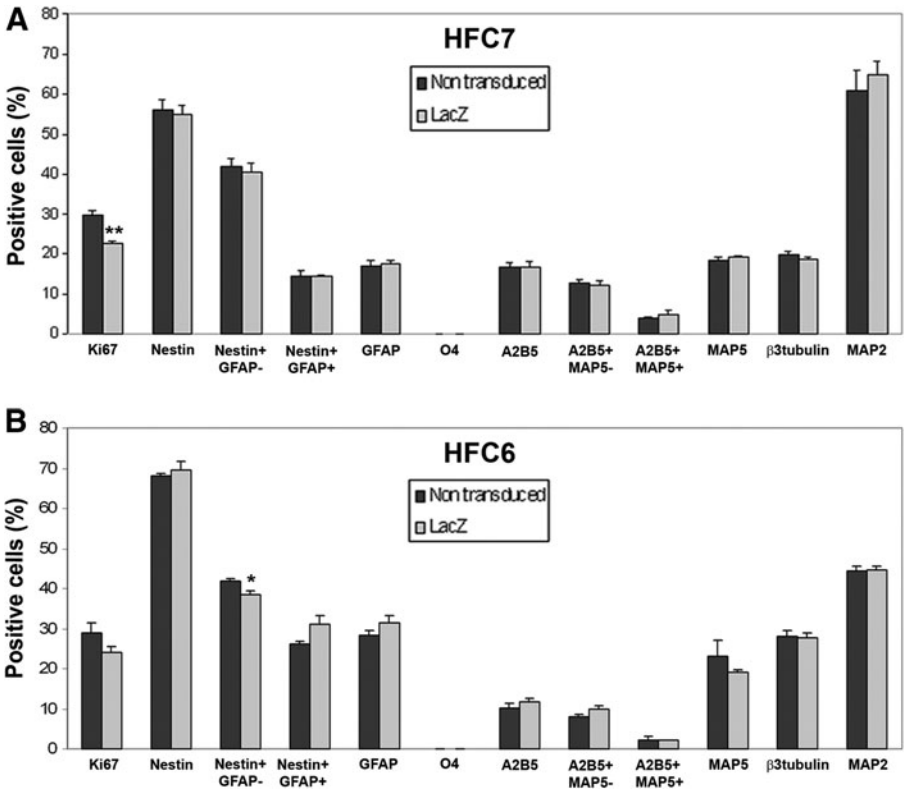

SUPPLEMENTARY FIG. S2. Transduction of HFC7 and HFC6 cells with a VSV-PGK-LacZ vector displays minor effects on the composition of the cell population. **(A, B)** Four days after transduction with a VSV-PGK-LacZ vector, comparison of naive and transduced HFC7 **(A)** and HFC6 **(B)** cells did not highlight any significant difference in the proportions of cells expressing most of the marker tested. Only a slight decrease in the proportion of Ki67+ proliferating cells **(A)** and in the proportion of Nestin +/GFAP-immature cells **(B)** was observed in the HFC7 and HFC6 cell populations, respectively. Proportions of positive cells are expressed as a percentage of total cell number ± SEM. Student's *t*-test: $*P < 0.05$; $**P < 0.01$.

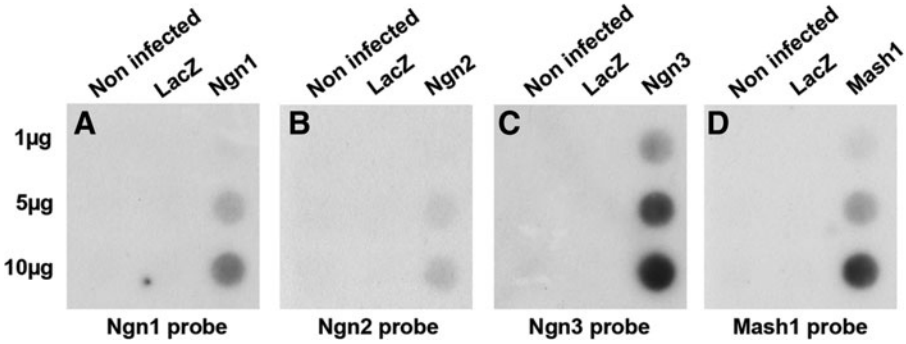

SUPPLEMENTARY FIG. S3. Lentiviral vectors efficiently transduce hNPCs. Dot blot analysis of proneural gene-encoding vector transduction efficiency. Human NPCs were transduced with the VSV-PGK-Ngn1 **(A)**, VSV-PGK-Ngn2 **(B)**, VSV-PGK-Ngn3 **(C)**, and VSV-PGK-Mash1 **(D)** vectors. Nontransduced hNPCs and hNPCs transduced with the VSV-PGK-LacZ vector were used as controls. Growing quantities of RNA extracts (1, 5, and 10 µg) were deposited on the membranes and incubated with a probe against each proneural gene tested. The presence of growing concentrations of Ngn1, Ngn2, Ngn3, and Mash1 RNA indicated that proviral DNA was inserted into the human genome and that the cellular machinery was used to carry out proneural gene transcription.

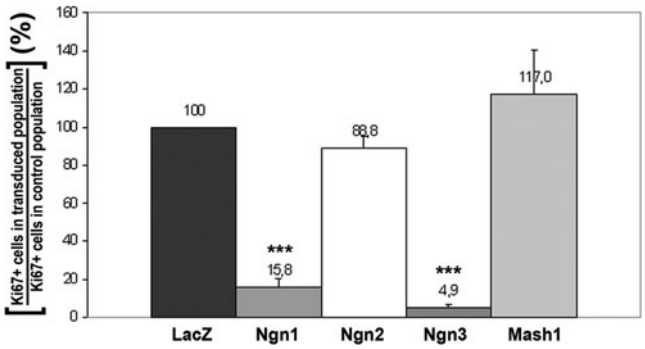

SUPPLEMENTARY FIG. S4. Overexpression of Ngn1 and Ngn3 in HFC6 cell population decreases the proportion of proliferating cells, whereas Mash1 does not affect proliferation. Impact of proneural gene overexpression on proliferation, expressed as the relative quantity of $Ki67^+$ proliferating cells in transduced populations (lacZ, Ngn1, Ngn2, Ngn3, and Mash1) reported on the quantity of $Ki67^+$ proliferating cells in the control LacZ population. Proliferation underwent a highly significant decrease after Ngn1 and Ngn3 overexpression, with an 84.2% and 95.1% reduction of $Ki67^+$ cells, respectively. The same tendency was observed after Ngn2 overexpression, although no significant differences were found. No differences in cell proliferation were highlighted after Mash1 overexpression. Student's *t*-test: $^{***}P < 0.001$.

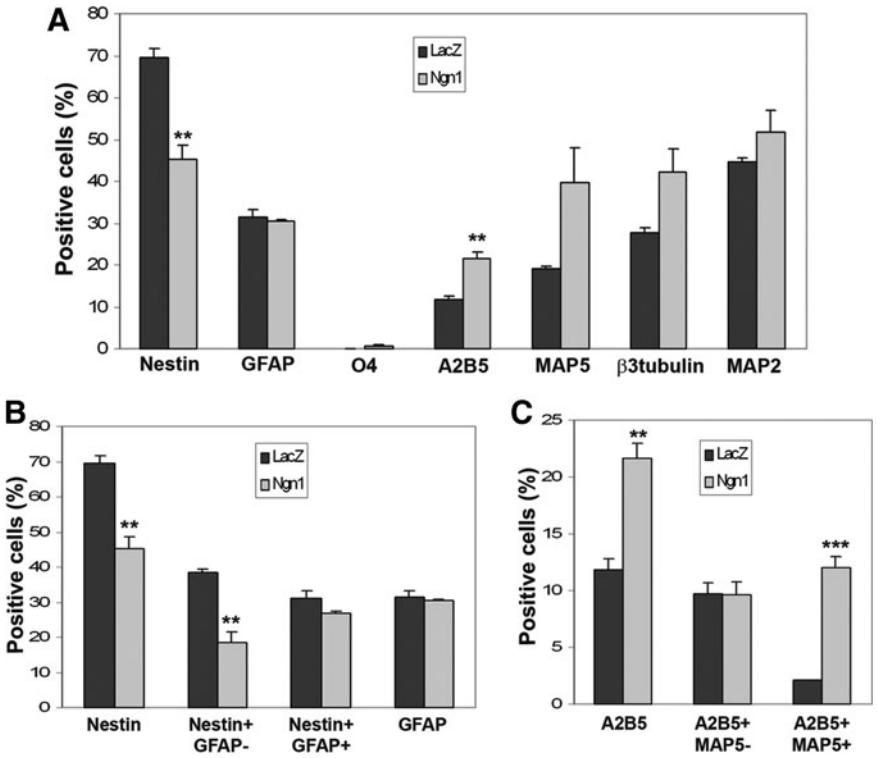

SUPPLEMENTARY FIG. S5. Ngn1 displays its proneural activity on HFC6 cells without affecting glial pathways. **(A–C)** Proportions of HFC6 cells from different neural lineages at 4 days after transduction with the VSV-PGK-LacZ and VSV-PGK-Ngn1 vectors. **(A)** Overexpression of Ngn1 induced a very significant decrease in the proportion of Nestin$^+$ cells, together with a very significant increase in the proportion of A2B5$^+$ cells. The proportions of MAP5$^+$ and β3 Tubulin$^+$ neuroblasts tended to increase, although no significant differences were highlighted between the 2 groups. Ngn1 overexpression did not affect the proportions of GFAP$^+$ astrocytes, O4$^+$ oligodendrocytes, and MAP2$^+$ mature neurons. **(B)** The decrease in the proportion of Nestin$^+$ cells reflected a very significant decrease in the proportion of Nestin$^+$/GFAP$^-$ neuroepithelial cells exclusively. Ngn1 overexpression did not affect the proportions of Nestin$^+$/GFAP$^+$ astrocytes. **(C)** The increase in the proportion of A2B5$^+$ cells reflected a highly significant increase in the proportion of A2B5$^+$/MAP5$^+$ neuroblasts exclusively. Ngn1 overexpression did not affect the proportion of A2B5$^+$/MAP5$^-$ OPCs. Student's *t*-test: $^{**}P < 0.01$; $^{***}P < 0.001$.

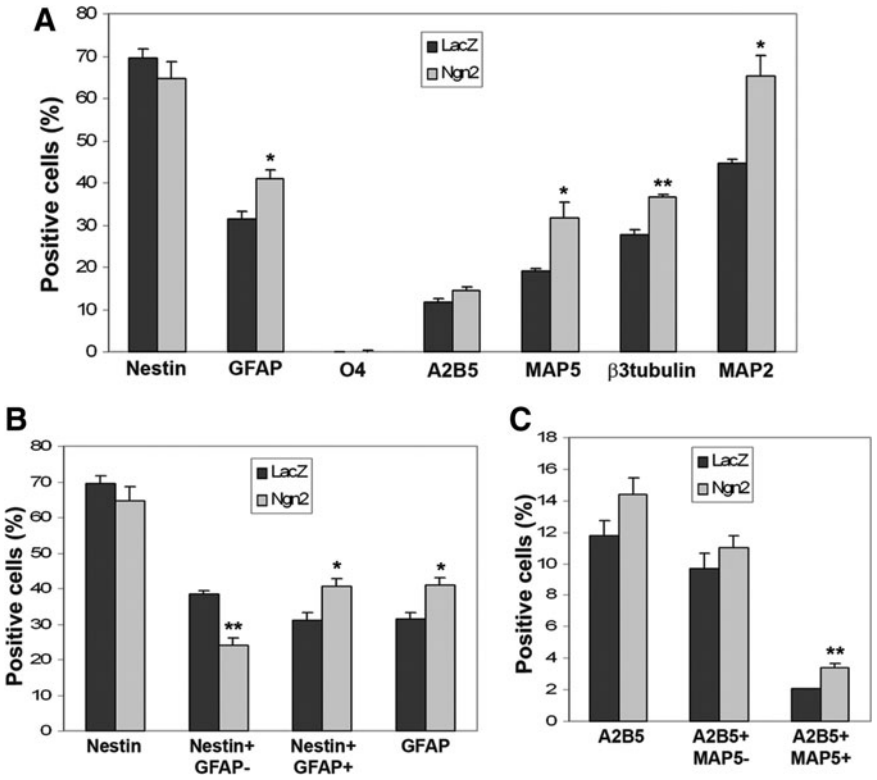

SUPPLEMENTARY FIG. S6. Ngn2 overexpression affects both neuronal and astroglial pathways in HFC6 cells. **(A–C)** Proportions of HFC6 cells from different neural lineages at 4 days after transduction with the VSV-PGK-LacZ and VSV-PGK-Ngn2 vectors. **(A)** Overexpression of Ngn2 did not affect the global proportion of Nestin$^+$ cells but induced a significant increase in the proportions of GFAP$^+$ astrocytes, MAP5$^+$ neuroblasts, and MAP2$^+$ mature neurons, together with a very significant increase in the proportions of β3 Tubulin$^+$ neuroblasts. **(B)** The global lack of changes in the proportion of Nestin$^+$ cells contrasted with the effects of Ngn2 overexpression on the neuroepithelial and astroglial cell populations. Overexpression of Ngn2 induced a very significant decrease in the proportion of Nestin$^+$/GFAP$^-$ neuroepithelial cells, along with a significant increase in the proportion of Nestin$^+$/GFAP$^+$ astrocytes. **(C)** The proportion of A2B5$^+$ cells globally tended to increase after Ngn2 overexpression, albeit without significance. Nevertheless, the proportion of A2B5$^+$/MAP5$^+$ neuroblasts underwent a very significant increase after Ngn2 overexpression, whereas the proportion of A2B5$^+$/MAP5$^-$ OPCs was not affected. Student's *t*-test: $^*P < 0.05$; $^{**}P < 0.01$.

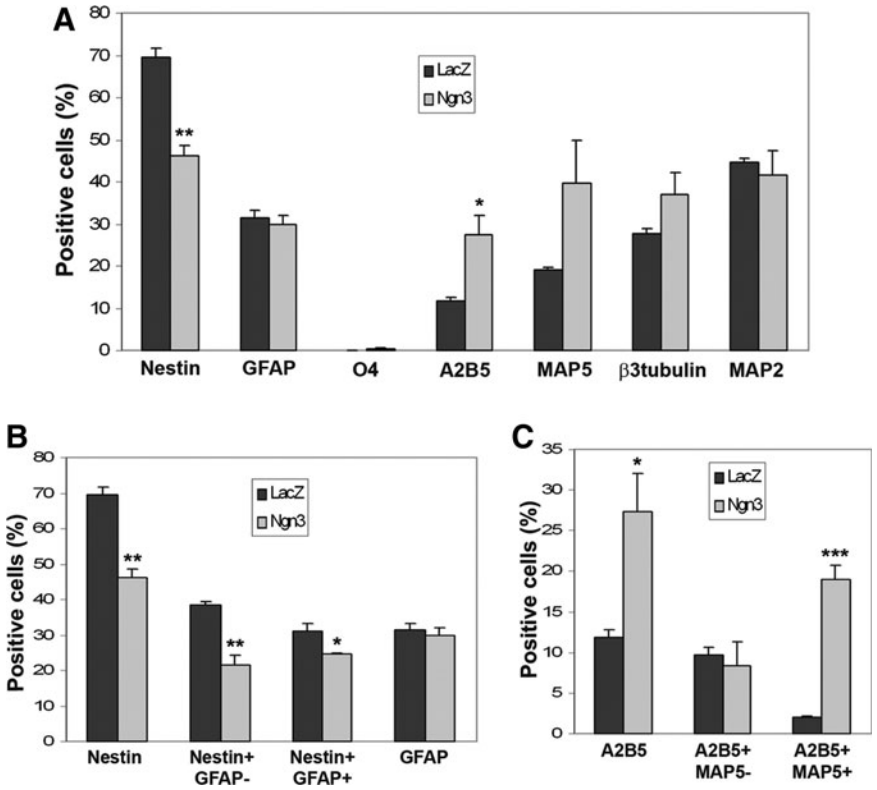

SUPPLEMENTARY FIG. S7. Ngn3 displays its proneural activity on HFC7 cells without affecting glial pathways. **(A–C)** Proportions of HFC6 cells from different neural lineages at 4 days after transduction with the VSV-PGK-LacZ and VSV-PGK-Ngn3 vectors. **(A)** Overexpression of Ngn3 induced a very significant decrease in the proportion of Nestin$^+$ cells, together with a significant increase in the proportions of A2B5$^+$ cells. The proportions of MAP5$^+$ and β3 Tubulin$^+$ neuroblasts tended to increase, although no statistical significance was highlighted. Ngn3 overexpression did not affect the proportions of GFAP$^+$ astrocytes, O4$^+$ oligodendrocytes, and MAP2$^+$ mature neurons. **(B)** The decrease in the proportion of Nestin$^+$ cells reflected both a very significant decrease in the proportion of Nestin$^+$/GFAP$^-$ neuroepithelial cells and a significant decrease in the proportion of Nestin$^+$/GFAP$^+$ astrocytes. However, the global proportion of GFAP$^+$ astrocytes was not affected by Ngn3 overexpression. **(C)** The increase in the proportion of A2B5$^+$ cells reflected a highly significant increase in the proportion of A2B5$^+$/MAP5$^+$ neuroblasts. However, Ngn3 overexpression did not affect the proportion of A2B5$^+$/MAP5$^-$ OPCs. Student's *t*-test: $^*P < 0.05$; $^{**}P < 0.01$; $^{***}P < 0.001$.

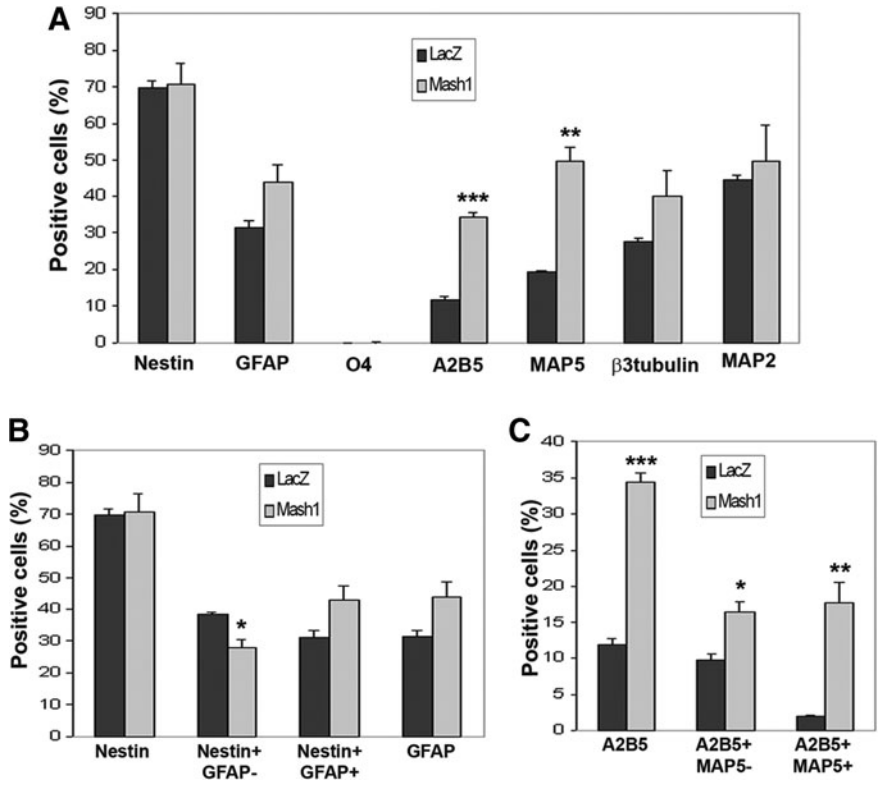

SUPPLEMENTARY FIG. S8. Mash1 overexpression in HFC6 cells promotes both neuronal and oligodendroglial specification. **(A–C)** Proportions of HFC6 cells from different neural lineages at 4 days after transduction with the VSV-PGK-LacZ and VSV-PGK-Mash1 vectors. **(A)** Overexpression of Mash1 did not affect the global proportions of Nestin$^+$ cells, but induced a highly significant increase in the proportion of A2B5$^+$ cells and a very significant increase in the proportion of MAP5$^+$ neuroblasts. No significant effect of Mash1 overexpression in HFC6 cells was highlighted on the proportions of GFAP$^+$ astrocytes, β3 Tubulin$^+$ neuroblasts, and MAP2$^+$ mature neurons. Most insterestingly, scarce O4$^+$ oligodendrocytes appeared as soon as 4 days after Mash1 overexpression. **(B)** Among Nestin$^+$ cells, the proportion of Nestin$^+$/GFAP$^-$ neuroepithelial cells underwent a significant decrease, whereas the proportion of Nestin$^+$/GFAP$^+$ astrocytes was not affected. **(C)** The increase in the proportion of A2B5$^+$ cells reflected both a very significant increase in the proportion of A2B5$^+$/MAP5$^+$ neuroblasts and a significant increase in the proportion of A2B5$^+$/MAP5$^-$ OPCs. Therefore, Mash1 overexpression induced both neuronal and oligodendroglial specification from HFC7 cells. Student's *t*-test: $^*P < 0.05$; $^{**}P < 0.01$; $^{***}P < 0.001$.

Supplementary Table S1. Statistics

	t(non-transduced, lacZ)	P	*t(lacZ, Ngn1)*	P	*t(lacZ, Ngn2)*	P	*t(lacZ, Ngn3)*	P	*t(lacZ, Mash1)*	P
HFC7										
Ki67	4.549	0.01	37.47	<0.001	12.569	<0.001	35.016	<0.001	0.0466	0.965
Nestin	0.427	0.691	5.133	0.007	0.355	0.247	8.868	<0.001	0.9	0.419
GFAP	−0.39	0.716	−1.519	0.203	−10.631	<0.001	2.378	0.076	0.081	0.939
$Nes^+/GFAP^+$	−0.0135	0.99	−1.933	0.125	−14.808	<0.001	7.122	0.002	0.306	0.775
$Nes^+/GFAP^-$	0.491	0.649	8.52	0.001	4.634	0.01	7.975	0.001	0.986	0.38
O4	0	1	0	1	0	1	−1.844	0.139	−1.292	0.266
A2B5	−0.0161	0.988	−5.898	0.004	−4.192	0.014	−4.95	0.008	−8.612	<0.001
$A2B5^+/MAP5^-$	0.371	0.729	−1.266	0.274	−0.457	0.671	−2.36	0.078	−4.724	0.009
$A2B5^+/MAP5^+$	−0.485	0.653	−5.057	0.007	−4.907	0.008	−6.035	0.004	−9.655	<0.001
MAP5	−0.704	0.52	−3.659	0.022	−3.432	0.026	−5.324	0.006	−9.681	<0.001
β3 tubulin	0.648	0.552	−8.306	0.001	−9.155	<0.001	−4.171	0.014	−2.802	0.049
MAP2	−0.697	0.524	0.17	0.873	−3.423	0.027	3.455	0.026	8.756	<0.001
HFC6										
Ki67	1.942	0.124	11.539	<0.001	1.716	0.161	14.547	<0.001	−0.691	0.528
Nestin	−0.748	0.496	5.86	0.004	1.116	0.327	7.39	0.002	−0.185	0.863
GFAP	−1.321	0.257	0.405	0.706	−3.312	0.03	0.486	0.652	−2.413	0.073
$Nes^+/GFAP^+$	−2.446	0.071	2.136	0.1	−3.141	0.035	3.279	0.031	−2.303	0.083
$Nes^+/GFAP^-$	3.272	0.031	6.202	0.003	6.494	0.003	6.119	0.004	4.113	0.015
O4	0	1	−1.506	0.206	−1	0.374	−1.458	0.219	−1.971	0.12
A2B5	−1.118	0.326	−5.983	0.004	−1.85	0.138	−3.19	0.033	−12.966	<0.001
$A2B5^+/MAP5^-$	−1.538	0.199	0.0701	0.947	−1.036	0.359	0.438	0.684	−4.122	0.015
$A2B5^+/MAP5^+$	0.0339	0.975	−10.972	<0.001	−5.12	0.007	−9.488	<0.001	−5.68	0.005
MAP5	0.965	0.389	−2.485	0.068	−3.103	0.036	−2.031	0.112	−7.467	0.002
β3 tubulin	0.0566	0.958	−2.621	0.059	−8.52	0.001	−1.786	0.149	−1.794	0.147
MAP2	−0.292	0.785	−1.388	0.238	−4.015	0.016	0.513	0.635	−0.502	0.642

Statistics have been performed using the Student's *t*-test to assess the effects of transduction with the VSV-PGK-lacZ, VSV-PGK-Ngn1, VSV-PGK, Ngn2, VSV-PGK-Ngn3, and VSV-PGK-Mash1 vectors on each marker tested. The phenotype of nontransduced HFC7 cells (*upper table*) and HFC6 cells (*lower table*) has been compared with that of HFC7 and HFC6 cells transduced with the VSV-PGK-lacZ vector. The phenotype of hNPCs transduced with the VSV-PGK-Ngn1, VSV-PGK, Ngn2, VSV-PGK-Ngn3, and VSV-PGK-Mash1 vectors has been compared with that of hNPCs transduced with the VSV-PGK-lacZ vector. HFC, human fetal cortex; hPNC, human neural progenitor cell; VSV, vesicular stomatitis virus envelope glycoprotein; PGK, phosphoglycerate kinase.